

Secular variation of Nd and Pb isotopes in ferromanganese crusts from the Atlantic, Indian and Pacific Oceans

R.K. O’Nions^{*}, M. Frank, F. von Blanckenburg¹, H.-F. Ling²

Department of Earth Sciences, University of Oxford, Parks Road, Oxford OX1 3PR, UK

Received 16 July 1997; revised 10 November 1997; accepted 10 November 1997

Abstract

Two ferromanganese crusts from the Indian Ocean and one from the Atlantic Ocean have been analysed for $^{10}\text{Be}/^9\text{Be}$, $^{143}\text{Nd}/^{144}\text{Nd}$ and $^{208,207,206}\text{Pb}/^{204}\text{Pb}$ ratios as a function of depth beneath their growth surfaces. $^{10}\text{Be}/^9\text{Be}$ ratios provide growth rate estimates for these crusts between 1.55 and 2.82 mm Ma^{-1} and further suggest that $^{87}\text{Sr}/^{86}\text{Sr}$ in crusts do not in any case examined so far provide reliable estimates for growth rates. A crust ALV-539 from 35°N in the western N. Atlantic has ϵ_{Nd} and Pb-isotope variations indistinguishable from crust BM-1969.05 from 39°N in the N. Atlantic [K.W. Burton, H.-F. Ling, R.K. O’Nions, Closure of the central American isthmus and its impact on North Atlantic deepwater circulation, *Nature* (London) 386 (1997) 382–385] when $^{10}\text{Be}/^{10}\text{Be}$ ratios are used to estimate growth rates. Both crusts provide evidence for a marked change in deepwater composition in the western N. Atlantic with a reduction in ϵ_{Nd} and an increase in $^{206}\text{Pb}/^{204}\text{Pb}$ from ~8 Ma ago towards the present day. The two crusts from the Indian Ocean show comparatively small variations in ϵ_{Nd} between -8.0 and -7.0 over the last 20 Ma and do not show the large shift in ϵ_{Nd} seen in the Atlantic crusts. Comparison of ϵ_{Nd} in the crusts analysed here with those published previously [H.-F. Ling, K.W. Burton, R.K. O’Nions, B.S. Kamber, F. von Blanckenburg, A.J. Gibb, J.R. Hein, Evolution of Nd and Pb isotopes in central Pacific seawater from ferromanganese crusts, *Earth Planet. Sci. Lett.* 146 (1997) 1–12; K.W. Burton, H.-F. Ling, R.K. O’Nions, Closure of the central American isthmus and its impact on North Atlantic deepwater circulation, *Nature* (London) 386 (1997) 382–385] shows that provinciality in the present-day ϵ_{Nd} structure of the Pacific, Atlantic and Indian Oceans has been maintained over ~20 Ma or more despite the palaeogeographic changes that have occurred within this period. These include the closure of the Panama gateway and the uplift of the Himalayas. Superimposed on this broad inter-ocean structure are changes in ϵ_{Nd} of the western N. Atlantic which may relate to the Panama gateway closure and shifts in the ϵ_{Nd} of equatorial Pacific deepwater from 3–5 Ma ago. The absence of any such structure in ϵ_{Nd} of the southwest and central Indian Ocean suggests that Himalayan erosion products such as preserved in the Bengal Fan sediments have not contributed significantly to Indian Ocean deepwater over the last 20 Ma. There is no straightforward relationship between records of $^{87}\text{Sr}/^{86}\text{Sr}$ in the global ocean and ϵ_{Nd} in ocean deepwater as would be expected if inputs of radiogenic Sr and unradiogenic Nd were coupled. © 1998 Elsevier Science B.V.

Keywords: neodymium; lead; isotopes; deep-water environment; Atlantic Ocean; Indian Ocean; Pacific Ocean

^{*} Corresponding author. E-mail: keitho@earth.ox.ac.uk

¹ Present address: Labor für Isotopengeologie, Universität Bern, Erlachstrasse 9a, CH-3012 Bern, Switzerland.

² Present address: Department of Earth Sciences, Nanjing University, Nanjing 210008, P.R. China.

1. Introduction

Natural radiogenic isotope tracers in seawater, such as ^{87}Sr , ^{143}Nd and $^{208,207,206}\text{Pb}$ are of particular value in the study of ocean circulation and mixing. This utility derives from their very different residence times in seawater and therefore their contrasting behaviour on the timescales of ocean circulation, and mixing. Thus Sr with a long residence time of ~ 2 Ma is isotopically well-mixed globally in the oceans. Although global mixing timescales for the oceans are not usually specified, it is assumed that substantial mixing accompanies ocean circulation which has a timescale around 10^3 a [1]; this is several orders of magnitude shorter than the timescale for Sr residence in the oceans. On the other hand, Nd and Pb which have shorter residence times estimated at ~ 1800 and ~ 80 a respectively [2–4] are not well-mixed in the oceans, and their isotopic distributions reflect erosional and hydrothermal inputs as well as different advective length scales accompanying ocean circulation.

These aspects of Sr, Nd and Pb behaviour in seawater have been exploited over a number of years both in studies of the provenance of these elements (e.g., [5–11] and also in the investigation of water mass movements in the South Atlantic [12] and the Antarctic circumpolar current [7,8,13]. Various attempts have been made to reconstruct secular changes in seawater Nd at specific points in the oceans, notable amongst which are the studies of Nd in foraminifera and their coatings [12,14]. Hydrogenous ferromanganese crusts have been shown to preserve records of seawater Nd and Pb which are recoverable on the million year timescale up to and beyond 20 Ma [15–17]. Results for a crust from 39°N in the W. North Atlantic [16] suggest a dramatic change in the Nd- and Pb-isotope composition of Atlantic deepwater between ~ 5 Ma and the present day. Three crusts formed in Pacific deepwater separated by ~ 2000 km also show significant changes in Nd-isotope composition over this same time interval [15]. The possibility has been raised that these variations are related in some way to the closing of the Panama gateway and the resulting restriction on exchange of seawater between the Pacific and Atlantic. The absence of a clear response to this gateway change in the Pacific deepwater Pb-isotope composition, con-

trasts with the marked change in Pb-isotope composition of western N. Atlantic deepwater particularly over the last 5 Ma. This presumably reflects a smaller advective length scale for Pb compared to Nd [15], as might be expected from its shorter residence times.

Although many general features of the global ocean circulation pattern are well understood, there remains considerable uncertainty about the nature of interbasin exchange and the detailed form of the flow. The simplified models of the ocean circulation pattern proposed by Broecker and Denton [18], Gordon [19] and Schmitz [20] for example, all emphasise laminar flow and the existence of a single global circulation cell. This view is challenged by the inversion of hydrographic data carried out by McDonald and Wunsch [21], which suggests that the system is better represented by two nearly independent cells, in which turbulent flow has an important role. Given the uncertainty about the present-day flow and circulation pattern of the oceans, prediction of the circulation patterns that accompanied alternative palaeogeographies such as existed for example when the Panama gateway was open or the Drake Passage restricted, must inevitably have severe limitations. Nevertheless, investigations of the effects of these palaeogeographic changes through general circulation models have come to broadly similar conclusions [22] and predict major changes to the circulation pattern and climate.

With this background, the records of secular change in the seawater isotope tracers Nd and Pb, recoverable from ferromanganese crusts, play a key part in reconstructing the pattern of ocean circulation. With sufficient control on the chronology of these changes their relationship to changes in palaeogeography including the effects of gateways between ocean basins may be assessed. In this contribution, results are presented for Nd- and Pb-isotope measurements on ferromanganese crusts from the Atlantic and Indian Oceans for which chronologies have been obtained using $^{10}\text{Be}/^9\text{Be}$ ratios. These records extend back beyond 20 Ma ago and therefore include the period of Himalayan uplift, and the palaeogeographic changes that occurred to the Indonesian passage and the Panama gateway. Also included here are the results for a ferromanganese crust from 39°N in the W. North Atlantic that has

also been dated using $^{10}\text{Be}/^{9}\text{Be}$ ratios. This crust has preserved a record of Nd and Pb isotopes over the period of the Panama gateway closure and complements the published results for a crust from 35°N [16] in the western N. Atlantic.

2. Samples and methods

Three ferromanganese crusts, two from the Indian Ocean and one from the Atlantic Ocean, have been analysed for Be, Nd and Pb isotopes as part of this project. Their locations are shown in Fig. 1. Of the Indian Ocean samples SS-663 is from a depth of 5.3 km at 13°S , 76°E in the central Indian Basin and 109 D-C is from a depth between 5.2 and 5.7 km at 28°S , 61°E in the Madagascar Basin, SW Indian Ocean. The third crust ALV539 was recovered from a depth of 2.7 km at 35°N , 59°W in the NW Atlantic. In addition, $^{10}\text{Be}/^{9}\text{Be}$ ratios have been obtained for a depth profile from Atlantic crust BM 1969.05 for which Sr, Nd and Pb data have been reported previously [16]. After petrographic examination these crusts were sampled mechanically perpendicular to the layering, using procedures similar to those previously reported by Ling et al. [15]. Following digestion of the crusts Be, Nd and Pb were separated by ion exchange methods to a level of purity suitable

for isotopic analysis. The chromatographic separation procedures used for Be followed those described previously [23,24] and the measurement of $^{10}\text{Be}/^{9}\text{Be}$ ratios was performed using a hot-SIMS technique on ISOLAB [25] in which Be^{+} is sputtered using O^{-} at a temperature where the residual B in the Be sample has evaporated off. Some improvements in analytical technique have been made since the earlier published work [25]. These include miniaturisation of the chemistry for Be separation, reduction in sample size of crust aliquots analysed to 5 mg and an improvement in the reproducibility of the L2 standard $^{10}\text{Be}/^{9}\text{Be}$ ratio to $\pm 3\%$ (2σ).

Nd and Pb were separated from the same sample aliquots as used for Be and their isotopic analysis by TIMS closely follows procedures used previously [15,26].

3. Results

3.1. Be isotopes

$^{10}\text{Be}/^{9}\text{Be}$ ratios for Atlantic Ocean crust ALV 539 and Indian Ocean crust 109 D-C are presented in Table 1 together with those for Atlantic crust BM 1969.05 studied previously by Burton et al. [16]. The $^{10}\text{Be}/^{9}\text{Be}$ data are plotted as a function of depth

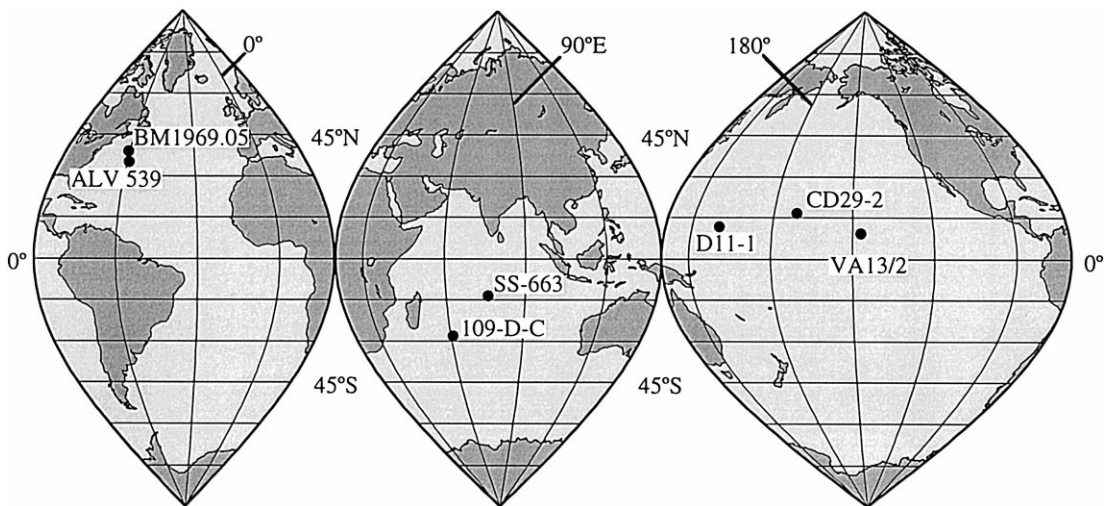


Fig. 1. World map showing the locations of the ferromanganese crusts studied. These are ALV-539 from the Atlantic Ocean, and SS-663 and 109 D-C from the Indian Ocean. Also shown are the locations of three Pacific crusts and one Atlantic crust studied previously [15,16].

Table 1
 $^{10}\text{Be}/^9\text{Be}$ ratios and ages of Fe–Mn crusts

Depth (m)	$^{10}\text{Be}/^9\text{Be} \pm 2\sigma^b$	Age ^c $\pm 2\sigma$ (Ma)
<i>BM 1969.05:</i>		
Surface ^a	$3.94 \pm 0.32 \times 10^{-8}$	0
0–1.0	$3.23 \pm 0.12 \times 10^{-8}$	0.43 ± 0.02
1.5–2.0	$2.19 \pm 0.25 \times 10^{-8}$	1.28 ± 0.15
2.5–3.0	$1.79 \pm 0.08 \times 10^{-8}$	1.72 ± 0.07
3.5–4.0	$1.41 \pm 0.06 \times 10^{-8}$	2.23 ± 0.10
4.0–5.0	$1.04 \pm 0.07 \times 10^{-8}$	2.90 ± 0.19
5.0–5.7	$9.00 \pm 0.52 \times 10^{-9}$	3.21 ± 0.19
5.7–6.0	$5.98 \pm 0.88 \times 10^{-9}$	4.10 ± 0.60
6.0–7.0	$5.20 \pm 0.44 \times 10^{-9}$	4.40 ± 0.37
8.0–8.5	$3.94 \pm 0.26 \times 10^{-9}$	5.01 ± 0.33
8.5–9.0	$2.69 \pm 0.62 \times 10^{-9}$	5.84 ± 1.34
9.0–10.0	$2.39 \pm 0.40 \times 10^{-9}$	6.09 ± 1.02
10.7–11.7	$1.85 \pm 0.44 \times 10^{-9}$	6.65 ± 1.58
<i>ALV 539:</i>		
0–1.0	$4.33 \pm 0.26 \times 10^{-8}$	0
1.5–2.0	$3.88 \pm 0.14 \times 10^{-8}$	0.24 ± 0.01
2.0–2.5	$3.46 \pm 0.14 \times 10^{-8}$	0.49 ± 0.02
2.5–3.0	$2.99 \pm 0.16 \times 10^{-8}$	0.81 ± 0.04
3.0–4.0	$2.58 \pm 0.09 \times 10^{-8}$	1.13 ± 0.38
4.0–5.0	$2.13 \pm 0.01 \times 10^{-8}$	1.54 ± 0.09
7.0–7.5	$1.74 \pm 0.34 \times 10^{-8}$	1.98 ± 0.39
7.5–8.5	$1.40 \pm 0.08 \times 10^{-8}$	2.45 ± 0.15
9.5–11.0	$6.59 \pm 0.56 \times 10^{-9}$	4.09 ± 0.35
12.0–13.5	$4.36 \pm 0.84 \times 10^{-9}$	4.99 ± 0.96
15.0–16.0	$2.42 \pm 0.20 \times 10^{-9}$	6.27 ± 0.53
18.0–19.0	$3.30 \pm 0.29 \times 10^{-9}$	5.59 ± 0.50
19.5–20.0	$4.36 \pm 0.64 \times 10^{-9}$	4.99 ± 0.73
20.8–22.2	$8.19 \pm 1.3 \times 10^{-10}$	8.63 ± 1.56
<i>109 D-C:</i>		
0–0.5	$9.46 \pm 0.35 \times 10^{-8}$	0
2.8–3.3	$4.97 \pm 0.18 \times 10^{-8}$	1.40 ± 0.05
5.5–6.0	$2.30 \pm 0.24 \times 10^{-8}$	3.08 ± 0.12
6.0–6.5	$1.87 \pm 0.08 \times 10^{-8}$	3.53 ± 0.17
8.5–9.0	$7.44 \pm 1.68 \times 10^{-9}$	5.53 ± 1.25
16.2–17.0	$6.74 \pm 0.61 \times 10^{-9}$	5.74 ± 0.52

^aSurface ratio after [23].

^bErrors include count statistical in-run precision and external reproducibility of 3% (2σ).

^cAges calculated using $\lambda^{10}\text{Be} = 0.46 \text{ Ma}^{-1}$.

beneath the present-day growth surface of crusts in Fig. 2. Growth rates for the crusts are estimated assuming that they have grown with the same $^{10}\text{Be}/^9\text{Be}$ ratio as measured at their present-day surface. These are 2.38 ± 0.15 , 1.55 ± 0.2 and 1.62

$\pm 0.1 \text{ mm Ma}^{-1}$ for ALV 539, 109 D-C and BM1969.05, respectively. Furthermore for crust 109 D-C the analysis from 15 mm depth in the crust has not been included in the growth rate estimate and it is assumed that this and two of the analysis points of ALV 539 have been subject to alteration. The growth rate of Indian Ocean crust SS 663 again based on $^{10}\text{Be}/^9\text{Be}$ ratios is $2.82 \pm 0.14 \text{ mm Ma}^{-1}$ similar to the other three crusts and data for this sample will be given by Frank et al. (in prep.). Overall, the growth rates for these Atlantic and Indian Ocean crusts are similar to those obtained for the central Pacific Ocean crusts [15], which are in the range 1.5–3.0 mm Ma^{-1} again using $^{10}\text{Be}/^9\text{Be}$ ratios with the assumption that the Pacific seawater source had a constant $^{10}\text{Be}/^9\text{Be}$ ratio throughout the growth of the crust. The timescales used in Figs. 3–5 are based on the extrapolation of $^{10}\text{Be}/^9\text{Be}$ -derived growth rates to the base of the crusts. Therefore, the uncertainties in the age estimates for the lower parts of the crusts are difficult to estimate objectively.

The estimate for the growth rate of Atlantic crust BM-1969.05 obtained here (Fig. 2) using $^{10}\text{Be}/^9\text{Be}$ ratios differs by about a factor of two from the earlier estimate based on $^{87}\text{Sr}/^{86}\text{Sr}$ ratios [16] and requires further comment. The $^{87}\text{Sr}/^{86}\text{Sr}$ profile obtained for this crust [16] is the only one measured so far in this laboratory which shows an internally consistent relationship to the seawater $^{87}\text{Sr}/^{86}\text{Sr}$ curve. However, even this crust now appears to give an erroneous result for reasons that are not yet clear. New $^{87}\text{Sr}/^{86}\text{Sr}$ ratios determined on crust ALV-539 (Table 2) are not reconcilable with the seawater $^{87}\text{Sr}/^{86}\text{Sr}$ curve either. At this stage it is prudent to view all crust chronologies based on $^{87}\text{Sr}/^{86}\text{Sr}$ ratios as only crude estimates at best.

3.2. Nd and Pb isotopes

3.2.1. Atlantic ALV 539

Nd and Pb isotope compositions for ALV 539 from the western N. Atlantic are presented in Table 2. ϵ_{Nd} values are quite uniform and range between -10.6 and -10.0 in the time interval 8–20 Ma (Fig. 3). However, from ~ 8 Ma to the present-day ϵ_{Nd} decreases from -10.6 to -13.0 ; this is towards

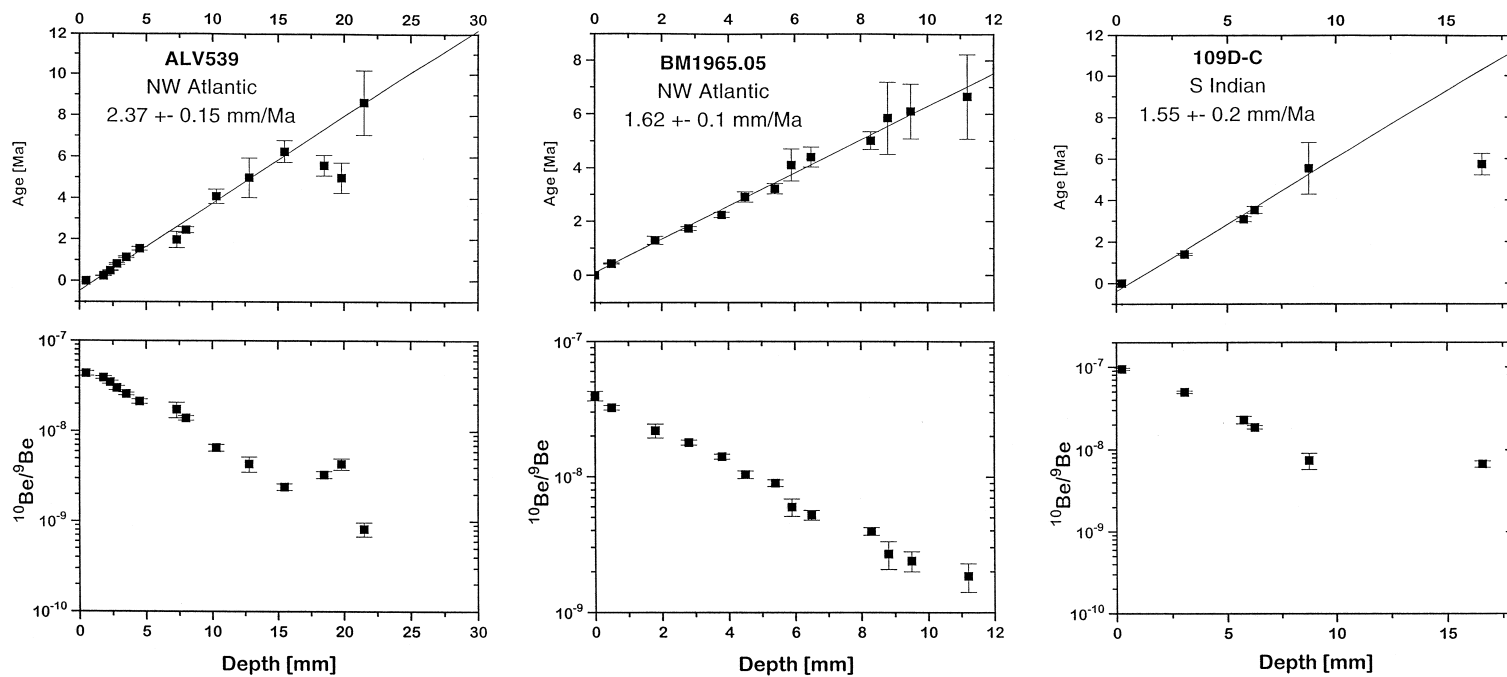


Fig. 2. $^{10}\text{Be}/^9\text{Be}$ ratios in ferromanganese crusts vs. depth beneath the growth surface. Growth rates are estimated assuming that the $^{10}\text{Be}/^9\text{Be}$ ratio has been constant at the growth surface of the crust. (a) Atlantic sample BM 1969.05; (b) Atlantic sample ALV-539; and (c) Indian Ocean sample 109 D-C. Sample locations are given in the text and Fig. 1.

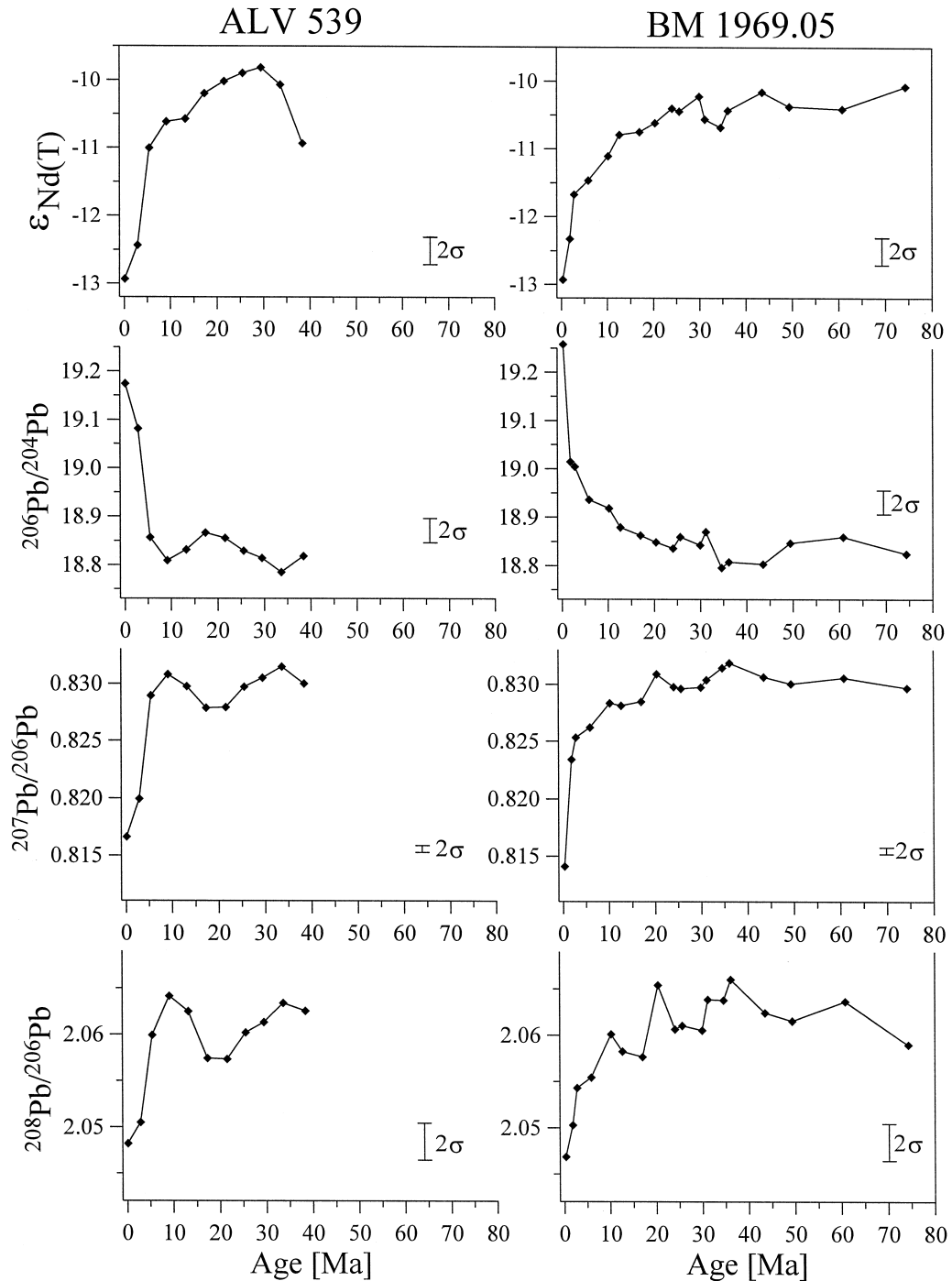


Fig. 3. Comparison of ϵ_{Nd} values, $^{206}Pb/^{204}Pb$, $^{207}Pb/^{206}Pb$ and $^{208}Pb/^{206}Pb$ ratios for Atlantic Ocean crusts ALV-539 (Table 2) and BM 1969.05 [16]. The time scales employed are derived from the $^{10}Be/^{9}Be$ ratios given in Fig. 2 and extrapolated assuming that the growth rates have been constant.

Table 2
Isotopic data of the crusts

Depth (mm)	Age ^a (Ma)	⁸⁷ Sr/ ⁸⁶ Sr ^b	¹⁴³ Nd/ ¹⁴⁴ Nd ^c	$\epsilon_{\text{Nd}}(0)$	$\epsilon_{\text{Nd}}(T)$ ^e	²⁰⁶ Pb/ ²⁰⁴ Pb ^d	²⁰⁷ Pb/ ²⁰⁴ Pb ^d	²⁰⁸ Pb/ ²⁰⁴ Pb ^d
<i>ALV539:</i>								
0–0.5	0.1	0.711086 ± 20	0.511975 ± 5	–12.93	–12.93 ± 0.10	19.174	15.658	39.273
6–7.5	2.8	0.709694 ± 11	0.511999 ± 5	–12.46	–12.44 ± 0.11	19.081	15.645	39.126
12–13.5	5.4	0.709053 ± 12	0.512071 ± 6	–11.06	–11.00 ± 0.11	18.857	15.631	38.843
20.8–22.2	9.1	0.708893 ± 10	0.512089 ± 6	–10.71	–10.61 ± 0.12	18.809	15.626	38.824
30.5–32	13.2	0.709021 ± 19	0.512089 ± 6	–10.71	–10.57 ± 0.11	18.831	15.625	38.839
40.2–41.8	17.3	0.708894 ± 15	0.512106 ± 6	–10.38	–10.20 ± 0.12	18.867	15.619	38.816
50.5–51.5	21.5	0.708830 ± 15	0.512113 ± 5	–10.24	–10.02 ± 0.10	18.856	15.611	38.791
59.8–61	25.5	0.708774 ± 15	0.512117 ± 6	–10.16	–9.90 ± 0.12	18.829	15.622	38.791
69–70.5	29.4	0.708771 ± 16	0.512119 ± 6	–10.12	–9.82 ± 0.12	18.814	15.625	38.781
78.8–80.3	33.6	0.709281 ± 15	0.512104 ± 5	–10.42	–10.07 ± 0.10	18.785	15.619	38.760
90.5–91.3	38.4	0.709349 ± 19	0.512057 ± 6	–11.33	–10.93 ± 0.12	18.818	15.619	38.813
<i>109 D-C:</i>								
0–0.5	0.2		0.512250 ± 4.4	–7.57	–7.57 ± 0.09	18.778	15.643	38.800
2.8–3.3	2.0		0.512230 ± 5	–7.96	–7.94 ± 0.10	18.815	15.643	38.819
5.5–6.0	3.7		0.512234 ± 5	–7.88	–7.84 ± 0.10	18.867	15.663	38.933
8.5–9.0	5.6		0.512222 ± 6	–8.11	–8.06 ± 0.12	18.868	15.668	38.953
13.5–14.8	9.1		0.512229 ± 5	–7.98	–7.88 ± 0.10	18.866	15.660	38.901
17.5–18.5	11.6		0.512226 ± 5.4	–8.04	–7.92 ± 0.11	18.888	15.666	38.992
21.0–21.5	13.7		0.512229 ± 5.4	–7.98	–7.84 ± 0.11	18.891	15.667	39.003
23.0–24.0	15.2		0.512230 ± 6	–7.96	–7.80 ± 0.12	18.868	15.658	38.959
26.5–26.8	17.2		0.512229 ± 6	–7.98	–7.80 ± 0.12	18.839	15.651	38.918
29.5–30.0	19.2		0.512235 ± 5.4	–7.86	–7.66 ± 0.11	18.882	15.653	38.974
<i>SS-663:</i>								
0.5–1.5	0.36		0.512266 ± 5	–7.26	–7.25 ± 0.10	18.890	15.703	39.133
7–8.5	2.77		0.512265 ± 7	–7.28	–7.25 ± 0.13	18.856	15.692	39.089
15–16.5	5.63		0.512276 ± 6	–7.06	–7.00 ± 0.11	18.829	15.695	39.095
22–23.5	8.13		0.512278 ± 5	–7.02	–6.94 ± 0.10	18.793	15.692	39.073
31.5–32.5	11.43		0.512250 ± 6	–7.57	–7.45 ± 0.12	18.737	15.677	38.999
41–42.5	14.91		0.512238 ± 6	–7.80	–7.65 ± 0.12	18.734	15.683	39.007
51–52.5	18.48		0.512232 ± 5	–7.92	–7.73 ± 0.10	18.585	15.626	38.696
58–60	21.07		0.512245 ± 6	–7.67	–7.45 ± 0.12	18.630	15.631	38.728
66–67	23.75		0.512231 ± 4	–7.94	–7.69 ± 0.08	18.653	15.630	38.740
70.5–71.5	25.36		0.512246 ± 5	–7.65	–7.38 ± 0.10	18.611	15.626	38.677

Samples from 109 D-C and SS-663 were dissolved without, and those from ALV 539 were dissolved after, acetic acid leaching. Errors given in the table are 2σ and based on within-run precision for individual mass spectrometer analyses. The external 2σ standard deviation of repeated runs of Sr, Nd and Pb standards during the period of this study are given below.

^aAges are calculated by extrapolation of growth rates defined by ¹⁰Be/⁹Be ratios in the outer parts of the crusts.

^b⁸⁷Sr/⁸⁶Sr normalised to ⁸⁶Sr/⁸⁸Sr = 0.1194; NBS-987 standard gave 0.710237 ± 0.000009 ($n = 7$).

^c¹⁴³Nd/¹⁴⁴Nd normalised to ¹⁴⁶Nd/¹⁴⁴Nd = 0.7219; JM-Nd standard yields 0.511118 ± 0.000008 ($n = 9$). La Jolla Nd yields 0.511858 ± 0.000010.

^dNBS-981 Pb standard yields ²⁰⁶Pb/²⁰⁴Pb = 16.899 ± 0.022; ²⁰⁷Pb/²⁰⁴Pb = 15.445 ± 0.023; ²⁰⁸Pb/²⁰⁴Pb = 36.554 ± 0.068 ($n = 26$).

Pb-isotope ratios in the table are presented after correction relative to the accepted value [30].

^e $\epsilon_{\text{Nd}}(T)$ values are calculated using ¹⁴⁷Sm/¹⁴⁴Nd = 0.115 [15].

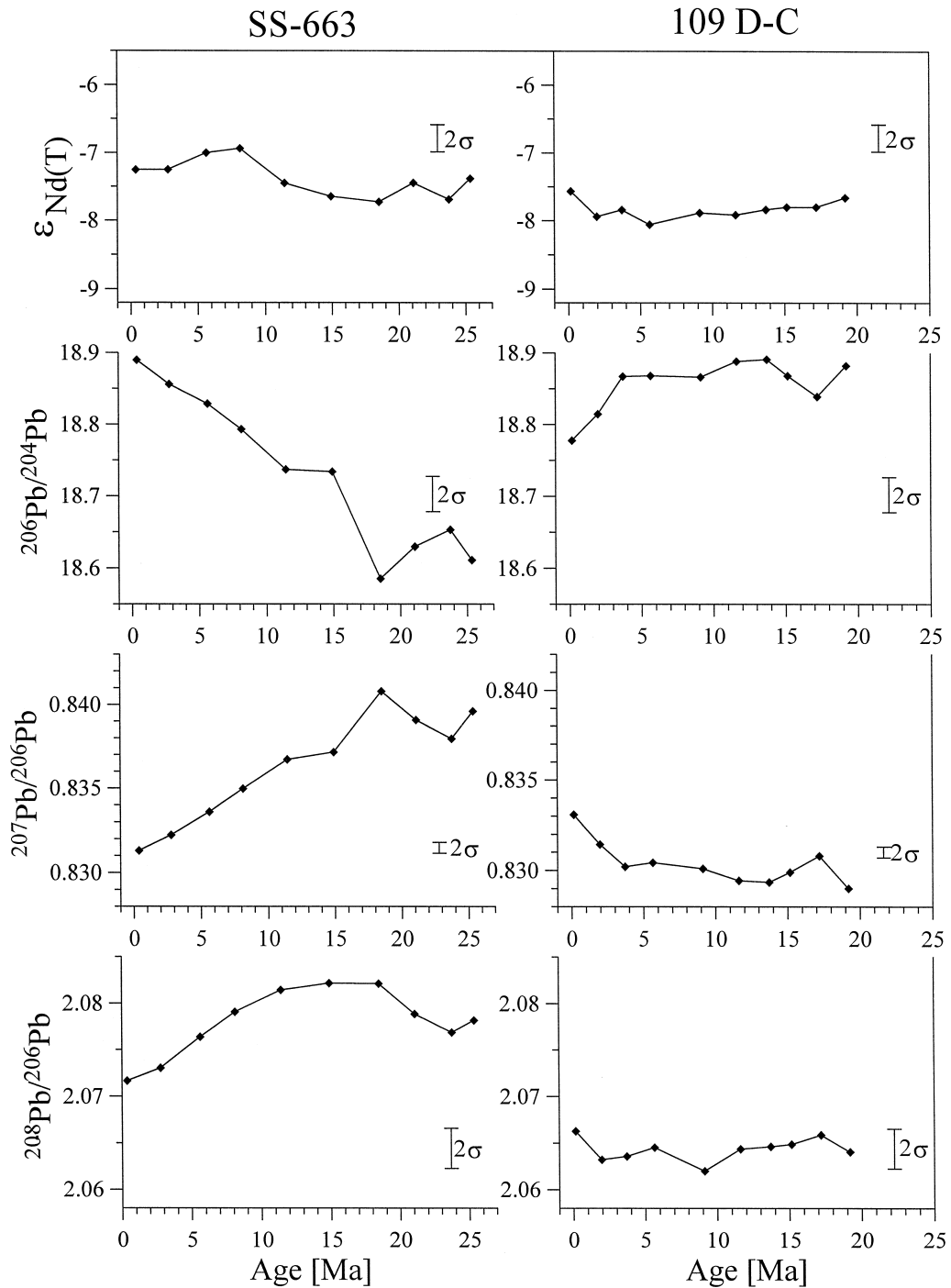


Fig. 4. Comparison ϵ_{Nd} values, $^{206}Pb/^{204}Pb$, $^{207}Pb/^{206}Pb$ and $^{208}Pb/^{206}Pb$ ratios for Indian Ocean crusts SS-663 and 109 D-C. The timescale for 109 D-C is from Fig. 2 and that for SS-663 will be given in Frank et al. (in prep.).

values more characteristic of the riverine input into the North Atlantic. The previously studied crust BM-1969.05 from 39°N in the W. North Atlantic [16], also shows a major shift in Nd-isotope composition by $-2 \epsilon_{\text{Nd}}$ units starting from $\sim 3\text{--}5$ Ma ago towards the present day using the old Sr chronology. This shift in Nd is paralleled by one in Pb with $^{206}\text{Pb}/^{204}\text{Pb}$, for example, increasing from ~ 18.84 prior to 3–5 Ma ago to 19.2 at the present day. However, the new chronology for this crust reported here (Table 1; Fig. 2) based upon $^{10}\text{Be}/^9\text{Be}$ ratios brings the Nd- and Pb-isotope structure in this Atlantic crust and BM-1969-05 (Fig. 3) into excellent agreement with the major change in deepwater composition starting ~ 8 Ma ago.

3.2.2. Indian SS-663 and 109 D-C

Nd- and Pb-isotope compositions for the two crusts from the Indian Ocean are given in Table 2 and Fig. 4. ϵ_{Nd} values in crust SS-663 from the central Indian Ocean (Fig. 1) vary between -7.7 and -7.0 over the thickness of the crust analysed. There is an indication of an overall decrease in ϵ_{Nd} with time but more data would be required to substantiate this. Crust 109 D-C from the SW Indian Ocean has similar ϵ_{Nd} values and these are within the range -8.1 to -7.5 , without any clearly resolved structure (Fig. 4). These results contrast with those from Atlantic crust ALV 539 (Fig. 3) and the previously published results for Atlantic and Pacific crusts (Figs. 3 and 6) which have well-resolved

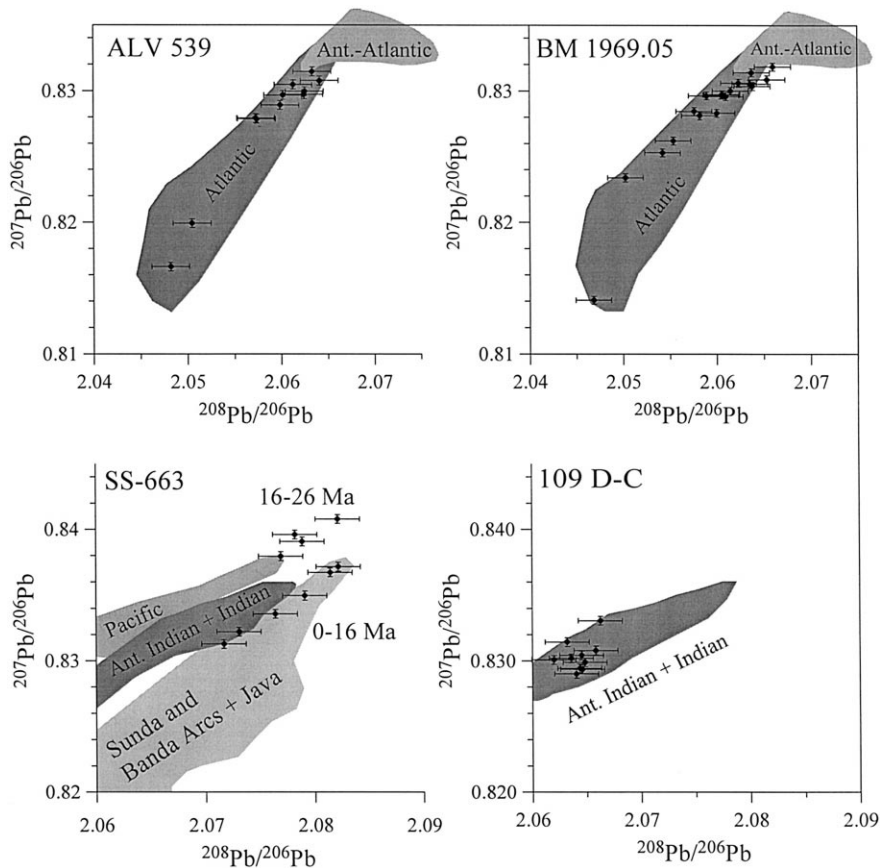


Fig. 5. Comparison of $^{207}\text{Pb}/^{206}\text{Pb}$ and $^{208}\text{Pb}/^{206}\text{Pb}$ ratios in Atlantic and Indian Ocean crusts. Note that the Atlantic samples ALV 539 and BM 1969.05 have $^{207}\text{Pb}/^{206}\text{Pb}$ and $^{208}\text{Pb}/^{206}\text{Pb}$ ratios within the range of published Pb data of modern Fe–Mn crust surfaces [11]. Indian Ocean crust SS 663 has Pb isotope ratios which show a secular change from Pacific-like values towards values similar to those in present-day Indonesian arc volcanics. The fields shown are based on published data from [7,11,27–29].

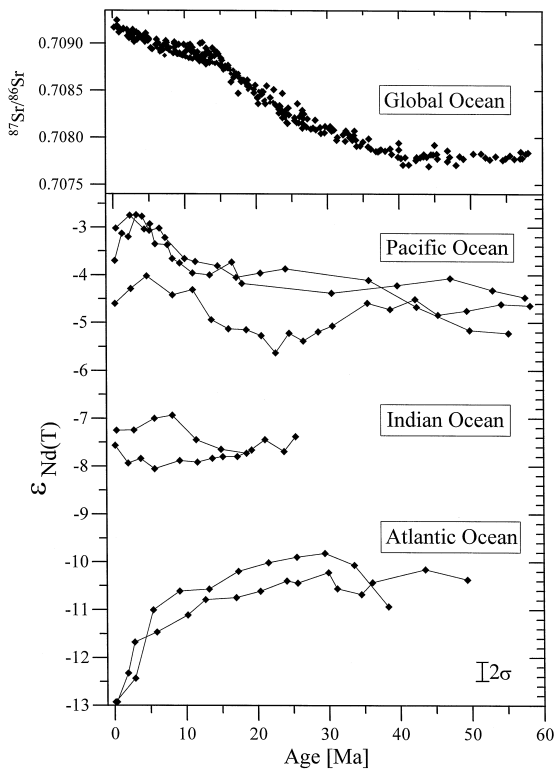


Fig. 6. Comparison of ϵ_{Nd} values in Pacific, Atlantic and Indian Ocean crusts based on $^{10}\text{Be}/^9\text{Be}$ chronology (this study and [15,16]) with the global ocean $^{87}\text{Sr}/^{86}\text{Sr}$ evolution. Sr data from [31–34].

structures in ϵ_{Nd} , particularly over the last 8 Ma. These two crusts from the Indian Ocean show no clearly resolved variations in ϵ_{Nd} over a 20 Ma period.

The Pb-isotope ratios obtained for the two Indian Ocean crusts show considerable differences (Table 2). $^{206}\text{Pb}/^{204}\text{Pb}$, $^{207}\text{Pb}/^{206}\text{Pb}$ and $^{208}\text{Pb}/^{206}\text{Pb}$ ratios for crust SS-663 and 109 D-C are compared in Fig. 4. Crust 109 D-C has a relatively constant $^{206}\text{Pb}/^{204}\text{Pb}$ ratio which is within the range 18.8–18.9 over the 20 Ma interval represented by sampling. Similarly, the $^{207}\text{Pb}/^{206}\text{Pb}$ and $^{208}\text{Pb}/^{206}\text{Pb}$ ratios for 109 D-C show no or only small variations. The $^{208}\text{Pb}/^{206}\text{Pb}$ ratios are within analytical error. In contrast, the Pb-isotope composition of SS-663 shows significant changes with time (Table 2). Thus $^{206}\text{Pb}/^{204}\text{Pb}$ ratios for this crust decrease from ~ 18.9 at the surface to ~ 18.6 at a depth correspond-

ing to 20 Ma. $^{207}\text{Pb}/^{206}\text{Pb}$ and $^{208}\text{Pb}/^{206}\text{Pb}$ ratios also vary considerably and increase from ~ 0.83 to ~ 0.84 and ~ 2.07 to ~ 2.08 , respectively, from the present day back to ~ 20 Ma ago (Fig. 4).

4. Discussion

4.1. Source of Nd and Pb in Indian ocean

Ferromanganese crusts 109 D-C and SS-663 were both dredged from depths greater than 5 km. They are expected therefore to have preserved a record of dissolved Nd and Pb in Indian Ocean deep- or bottomwater over a period of ~ 20 Ma.

At the present day deepwater in the southwest Indian Ocean at the location of 109 D-C in the Madagascar Basin appears to be supplied from circumpolar deepwater (CDW) [19,35]. Some $55 \times 10^6 \text{ m}^3 \text{ s}^{-1}$ of water are estimated to be transported as CDW of which $14 \times 10^6 \text{ m}^3 \text{ s}^{-1}$ leave CDW in the southwest Indian Ocean and $10 \times 10^6 \text{ m}^3 \text{ s}^{-1}$ leave CDW south of Australia [20] to form Indian Ocean Bottom Water (IOBW). This source alone is able to replenish the entire volume of Indian Ocean water ($2.8 \times 10^{17} \text{ m}^3$) in less than 500 a. The source of IOBW in the central Indian Ocean at the location of crust SS-663 is less straightforward. Most likely it is also supplied from CDW but in this case [20] water is exported to form IOBW south of Australia.

The ϵ_{Nd} values in the surfaces of the two Indian crusts are between -7.5 and -7.0 and are considered to have been derived from recent Indian deep- or bottomwater. It is interesting to note therefore that samples of manganese nodules from the southern Indian Ocean although poorly constrained chronologically do have ϵ_{Nd} values [8,13] broadly consistent with those for the two Indian Ocean crusts analysed here. This characteristic ϵ_{Nd} value is distinctly higher than the ϵ_{Nd} values in modern deepwater recovered from the North and South Atlantic ($-13 < \epsilon_{\text{Nd}} < -8$) [3,36], but lower than the ϵ_{Nd} values of around -4 obtained for Pacific Ocean deepwater [37,38]. It is consistent with a source which is a mixture between Pacific and Atlantic deepwaters which after mixing in CDW, is advected as bottomwater into the Indian Ocean. The replenishment time of Indian Ocean deepwater is fast enough

relative to the residence time of Nd so that in principle other sources of Nd need not necessarily be required to explain the Nd patterns observed.

An important question is whether Nd from sources other than CDW have contributed to deepwaters in the central and southwest Indian Ocean. Of particular interest is the role of Himalayan erosion either at the present day or in the past, given that the Himalayas have been considered to be an important source of ^{87}Sr supply to the oceans. However, the estimate for the ϵ_{Nd} value of Himalayan erosion products available from Bengal fan sediments produced over the last 10 Ma is around -15 [39]. This compares with the relatively uniform ϵ_{Nd} value between -7.5 and -7.0 for the crusts and suggests that the Himalayas have not been a major source of Nd to Indian Ocean deepwater. This result is perhaps surprising given the enormous amount of erosion of the Himalayas that has occurred over this time interval. There are several possibilities: (1) the sediment record within the Bengal Fan is atypical of Himalayan erosion products. Those entering the Indian Ocean had ϵ_{Nd} values closer to those recorded by the crusts; (2) Himalayan Nd only enters the surface waters of the Indian Ocean, which neither sink nor mix vertically to contribute Nd to IOBW; (3) dissolved riverine and particulate Nd from the Himalayas is retained within the fans or on the shelves and does not enter the ocean to a significant extent; and (4) there is one or more additional sources with ϵ_{Nd} greater than -7 which compensate for the Himalayan Nd input.

The first of these possibilities is difficult to evaluate but given the uniform ϵ_{Nd} value of the fan deposits [39] it seems unlikely that Nd with a very different composition could have entered the Indian along this same pathway. The second possibility that the Himalayan Nd is carried out of the Indian Ocean in surface waters is not supported by the measurements of ϵ_{Nd} in seawater samples from the western Indian [40]. Therefore the possibility that Nd is retained on particulates on the shelves and leads to a decoupling of the dissolved Sr and Nd load should be given serious consideration. Alternatively, it appears that a fortuitous balance between Himalayan and other sources of Nd which matches the ϵ_{Nd} value of the crusts must be entertained.

In contrast to the similar and relatively uniform ϵ_{Nd} values of the two Indian Ocean crusts (Figs. 4

and 6), Pb-isotope compositions differ significantly both at the present day and over the last 20 Ma (Fig. 4). Pb-isotope ratios of crust 109 D-C from the SW Indian Ocean vary little over ~ 20 Ma (Fig. 4) and are comparable to those reported for manganese nodules and crusts from the Antarctic region [7,11]. However, crust SS-663 from the central Indian shows a decrease in $^{206}\text{Pb}/^{204}\text{Pb}$ ratio from 18.9 to 18.6 and concomitant increases in both $^{208}\text{Pb}/^{206}\text{Pb}$ and $^{207}\text{Pb}/^{206}\text{Pb}$ ratios back to ~ 20 Ma ago. Inspection of their $^{207}\text{Pb}/^{206}\text{Pb}$ and $^{208}\text{Pb}/^{206}\text{Pb}$ ratios in Fig. 5 shows that three or more Pb components have been present at different times in the central Indian deepwater over the history of the crust. Overall there has been a change in the relative importance of sources with isotope characteristics more similar to the present-day Pacific towards one similar to potential sources of Pb in the Indonesian arcs (Fig. 5). In this regard it is significant that the Indonesian through-flow which might transport this Pb into the Indian Ocean is $\sim 10 \times 10^6 \text{ m}^3 \text{ s}^{-1}$ and that arcs have previously been suggested as major sources of Pb in the Pacific Ocean [11]. Although drainage from the Himalayas has not yet been characterised for Pb isotopes, it is entirely possible that Pb from this source is also present in IOBW and may play a role in the secular change of Pb isotopes in the central Indian Ocean. Thus whereas a well-mixed source of Nd in CDW may supply both regions, albeit via different routes [20], it does not necessarily follow that Pb will be the same in both locations because the advective length scales could be sufficiently different to cause some decoupling of Nd and Pb.

4.2. Indian, Pacific and Atlantic secular changes

The results presented in this paper when combined with published data [15,16] make a total of seven ferromanganese crusts for which $^{10}\text{Be}/^9\text{Be}$ chronologies and Nd- and Pb-isotope records exist. This includes three crusts from the central Pacific, two from the western North Atlantic and two from the Indian Ocean each of which have records of seawater Nd and Pb extending back to 20 Ma or more. Although the number of crusts is still small it is large enough to reveal some general features of the provinciality of Nd and the secular change of seawater Nd and Pb isotopes.

The ϵ_{Nd} records in Pacific, Atlantic and Indian Ocean crusts are compared in Fig. 6. The striking provinciality of ϵ_{Nd} in the present-day oceans — a feature which has been known for many years — is immediately evident. It is now clear that this provinciality has been maintained for the last 20 Ma and possibly much longer. It has been maintained despite the changes in palaeogeography that have occurred over the time interval represented by the crusts, including for example the final closure of the Panama gateway around 3–4 Ma ago [41], the opening of the Drake Passage around 23 Ma ago [42] and the closure of Tethys at ~ 12 Ma [43]. The samples available for this study may, however, be located too far away from the respective gateways to record a clear signal; it will be necessary to investigate samples from other locations closer to the gateways as part of a future study. The ϵ_{Nd} records may also be compared with the Sr-isotope record for the oceans over the same time interval (Fig. 6). It is immediately clear that the general increase in the $^{87}\text{Sr}/^{86}\text{Sr}$ ratio of the oceans over the last 10–15 Ma has not been accompanied by a parallel and global decrease in the ϵ_{Nd} value of the world's oceans as would be expected if they had received an increased and coupled supply of radiogenic Sr and unradiogenic Nd. One possibility is that Sr and Nd isotopes were decoupled during erosion and transport such that dissolved riverine radiogenic Sr was delivered to the oceans but the complementary Nd was retained on the continents or their shelves. Alternatively, the increase in ocean $^{87}\text{Sr}/^{86}\text{Sr}$ ratio did not occur through an increased input of Sr to the oceans with a high $^{87}\text{Sr}/^{86}\text{Sr}$ ratio but involved, for example, a reduction in the ridge flux of Sr with low $^{87}\text{Sr}/^{86}\text{Sr}$; the ridges being an insignificant source of Nd to the oceans.

These different responses to changes in provenance and circulation are illustrated by the Nd and Pb composition of the crusts. Within the fine structure of the secular variation in ϵ_{Nd} values (Fig. 6) the maintenance of a difference in the ϵ_{Nd} values in Pacific crusts at different water depths is striking. The crust from a depth of 4.8 km in the Pacific has been around 1.0 ϵ_{Nd} more negative than the crust from 1.8 km over a period of ~ 20 Ma or more. The long-term stratification of ϵ_{Nd} in the central Pacific Ocean inferred from the crusts requires that Nd in

the central Pacific Ocean has been supplied from two or more sources over the last 20 Ma or more. It further requires that Nd is transported from its point of input over basin scale distances by the ocean circulation. This requirement does not extend to Pb in the central Pacific due to its uniform composition, and there is no evidence for sources of Pb from outside the Basin. In contrast, the North Atlantic crusts show straightforward evidence from ~ 8 Ma ago for a change in source of Nd in the deepwater present in this part of the Atlantic. The entry point of Nd into the Atlantic was sufficiently close to 35°N that a coherent variation in Pb and Nd isotopes is recorded by the crusts from 8 Ma ago to the present day. Such phasing of Nd and Pb variations in seawater would not be expected after large flow distances from the place of input because the Pb signal would decay relative to the Nd signal.

The interplay of source control and ocean circulation on Nd and Pb is again seen in the Indian Ocean samples. Here the situation is quite different. In the central Indian crust SS-663 the Pb isotopes show a secular variation which is uncorrelated with Nd-isotope variation in the same sample and contrasts markedly with the relative uniformity of Pb isotopes in the second crust from the Madagascar Basin. This presumably reflects local changes in the provenance of Pb in the central Indian superimposed on a uniform ϵ_{Nd} profile which is a record of the Nd advected into the central Indian Ocean from CDW.

4.3. Timing of ϵ_{Nd} shifts in the Atlantic and Pacific

Both crusts from the Atlantic Ocean (Fig. 6) show a decrease by ~ 2 ϵ_{Nd} from ~ 8 Ma ago to the present day. This shift as noted above is in phase with a change in Pb isotopes over the same time interval. It records an increased availability of Nd and Pb derived from older continental crust for the deepwater sampled at $35\text{--}39^\circ\text{N}$ in the western N. Atlantic. Whether this arises from a relative increase in the input into the Atlantic from a particular continental source or alternatively from a change in N. Atlantic circulation is not determined. However, the start of the shift in ϵ_{Nd} towards more negative values around 8 Ma is much earlier than the onset of northern hemisphere glaciation and the changes in erosion that accompanied it. It is also earlier than

estimates for the time of strengthening of NADW. Nevertheless Nd and Pb which are most plausibly derived from a N. Atlantic continental source [16] were clearly present in deepwater between 35° and 39°N well prior to the onset northern hemisphere glaciation.

In contrast to the Atlantic, the equatorial Pacific crusts (Fig. 6) show a decrease in ϵ_{Nd} from 3–5 Ma ago rather than 8 Ma ago and then only by $\leq 1 \epsilon_{\text{Nd}}$ unit. Because the ocean circulation time is around 1500 a the changes in the Pacific and Atlantic ϵ_{Nd} cannot be directly related to a single change in erosional input. Indeed they could be related to the same erosion source only if circulation changes occurring around 3–5 Ma ago brought the NADW Nd signal into the Pacific. These and other possible scenarios for the shifts in ϵ_{Nd} and their relationship to the emergence of the Panama isthmus become important questions for the future.

5. Concluding remarks

The Be, Nd and Pb isotope records for three crusts reported here together with the four records already published [15,16] reveal some remarkable features about the behaviour of Nd and Pb in the oceans. There is a long-term provinciality in Nd isotopes in the Atlantic, Pacific and Indian Oceans, together with the stratification of ϵ_{Nd} in the equatorial Pacific, over ~ 20 Ma or more. These features and the superimposed shorter timescale variations are consistent with a Nd residence time which allows advection of Nd in deepwater within and between ocean basins. In contrast Pb because of its much shorter residence time responds more to local changes in provenance and only shows coherent variations with Nd in the western N. Atlantic samples. This is presumably because these sites are relatively close to the site of NADW generation in the N. Atlantic. If this interpretation is correct, then the coherent relationship between Nd and Pb isotopes is expected to break down and become decoupled as the NADW flow continues southwards into the S. Atlantic.

A puzzling aspect of the results is the absence of any clear shifts in the ϵ_{Nd} values of two Indian Ocean crusts which correlate with the major palaeogeographic changes that have occurred over the last 20 Ma, or indeed the uplift and erosion of the

Himalayas which have emplaced an enormous load of Nd with ϵ_{Nd} around -15 into the Indian Ocean. This is much lower than the -8.0 to -7.0 values observed in the two Indian crusts. One possibility is that this Nd has remained in the particulate load such as that deposited in the Bengal Fan with very little entering the Indian Ocean as part of the dissolved load.

Acknowledgements

This research has been supported by the Natural Environment Research Council and the EU. The manuscript was reviewed by Chris Hawkesworth and Stein Jacobsen. The authors are grateful to Jim Hein for the supply of samples for this study and to Andy Gibb and Yueling Guo for help with the mass spectrometry and chemistry. *[MKJ]*

References

- [1] W.S. Broecker, The great ocean conveyor, *Oceanography* 4 (1991) 79–89.
- [2] C. Jeandel, J.K. Bishop, A. Zindler, Exchange of neodymium and its isotopes between seawater and small and large particles in the Sargasso Sea, *Geochim. Cosmochim. Acta* 59 (1995) 535–547.
- [3] C. Jeandel, Concentration and isotopic composition of Nd in the South Atlantic Ocean, *Earth Planet. Sci. Lett.* 117 (1993) 581–591.
- [4] B.K. Schaule, C.C. Patterson, Lead concentration in the northeast Pacific: evidence for global anthropogenic perturbations, *Earth Planet. Sci. Lett.* 54 (1981) 97–116.
- [5] R.K. O'Nions, S.R. Carter, R.S. Cohen, N.H. Evensen, P.J. Hamilton, Pb, Nd and Sr isotopes in oceanic ferromanganese deposits and ocean floor basalts, *Nature (London)* 273 (1978) 435–438.
- [6] S.L. Goldstein, R.K. O'Nions, Nd and Sr isotopic relationships in pelagic clays and ferromanganese deposits, *Nature (London)* 292 (1981) 1–4.
- [7] W. Abouchami, S.L. Goldstein, A lead isotopic study of circum-Antarctic manganese nodules, *Geochim. Cosmochim. Acta* 59 (1995) 1809–1820.
- [8] F. Albarède, S.L. Goldstein, World map of Nd-isotopes in sea-floor ferromanganese deposits, *Geology* 20 (1992) 761–763.
- [9] G.W. Brass, The variation of the marine $^{87}\text{Sr}/^{86}\text{Sr}$ ratio during Phanerozoic time: interpretation using a flux model, *Geochim. Cosmochim. Acta* 40 (1976) 721–730.
- [10] L.A. Derry, C. France-Lanord, Neogene Himalayan weathering history and river $^{87}\text{Sr}/^{86}\text{Sr}$: impact on the marine Sr record, *Earth Planet. Sci. Lett.* 142 (1996) 59–74.

- [11] F. von Blanckenburg, R.K. O'Nions, J.R. Hein, Distribution and sources of pre-anthropogenic lead isotopes in deep ocean water from Fe–Mn crusts, *Geochim. Cosmochim. Acta* 60 (1996) 4957–4963.
- [12] M.R. Palmer, H. Elderfield, Rare-earth elements and neodymium isotopes in ferromanganese oxide coating of Cenozoic foraminifera from the Atlantic Ocean, *Geochim. Cosmochim. Acta* 50 (1986) 409–417.
- [13] F. Albarède, S.L. Goldstein, D. Dautel, The neodymium isotope composition of manganese nodules from the Southern and Indian Oceans, the global neodymium budget, and their bearing on ocean circulation, *Geochim. Cosmochim. Acta* 61 (1997) 1277–1292.
- [14] P. Stille, M. Steinmann, S.R. Riggs, Nd isotope evidence for the evolution of paleocurrents in the Atlantic and Tethys Oceans during the past 180 Ma, *Earth Planet. Sci. Lett.* 144 (1996) 9–19.
- [15] H.-F. Ling, K.W. Burton, R.K. O'Nions, B.S. Kamber, F. von Blanckenburg, A.J. Gibb, J.R. Hein, Evolution of Nd and Pb isotopes in central Pacific seawater from ferromanganese crusts, *Earth Planet. Sci. Lett.* 146 (1997) 1–12.
- [16] K.W. Burton, H.-F. Ling, R.K. O'Nions, Closure of the central American isthmus and its impact on North Atlantic deepwater circulation, *Nature (London)* 386 (1997) 382–385.
- [17] J.R. Christensen, A.N. Halliday, L.V. Godfrey, J.R. Hein, D.K. Rea, Climate and ocean dynamics and the lead isotopic records in Pacific ferromanganese crusts, *Science* 277 (1997) 913–918.
- [18] W.S. Broecker, G.H. Denton, The role of ocean–atmosphere re-organisations in glacial cycles, *Geochim. Cosmochim. Acta* 53 (1989) 2465–2501.
- [19] A.L. Gordon, Inter-ocean exchange of thermocline water, *J. Geophys. Res.* 91 (1986) 5037–5046.
- [20] W.J. Schmitz, On the inter-basin-scale thermohaline circulation, *Rev. Geophys.* 33 (1995) 151–173.
- [21] A.M. Macdonald, C. Wunsch, An estimate of global ocean circulation and heat fluxes, *Nature (London)* 382 (1996) 436–439.
- [22] E. Maier-Reimer, U. Mikolajewicz, T.J. Crowley, Ocean general circulation model sensitivity experiment with an open central American isthmus, *Paleoceanography* 5 (1990) 349–366.
- [23] F. von Blanckenburg, R.K. O'Nions, N.S. Belshaw, A. Gibb, J.R. Hein, Global distribution of beryllium isotopes in deep water as derived from Fe–Mn crusts, *Earth Planet. Sci. Lett.* 141 (1996) 213–226.
- [24] F. von Blanckenburg, N.S. Belshaw, R.K. O'Nions, Separation of ^9Be and cosmogenic ^{10}Be from environmental materials and SIMS isotope dilution analysis, *Chem. Geol.* 129 (1996) 93–99.
- [25] N.S. Belshaw, R.K. O'Nions, F. von Blanckenburg, A SIMS method for $^{10}\text{Be}/^9\text{Be}$ ratio measurements in environmental materials, *Int. J. Mass Spectrom. Ion. Phys.* 142 (1995) 55–67.
- [26] A.S. Cohen, R.K. O'Nions, R. Siegenthaler, W.L. Griffen, Chronology of the pressure–temperature history recorded by a granulite terrain, *Contrib. Mineral. Petrol.* 98 (1988) 303–311.
- [27] F. McDermott, C.J. Hawkesworth, Th, Pb, and Sr isotope variations in young island arc volcanics and oceanic sediments, *Earth Planet. Sci. Lett.* 104 (1991) 1–15.
- [28] A.J. Stolz, R. Varne, G.E. Wheller, J.D. Foden, Magma source components in an arc–continent collision zone; the Flores–Lembata sector, Sunda arc, Indonesia, *Contrib. Mineral. Petrol.* 105 (1990) 585–601.
- [29] P.Z. Vroon, M.J. van Bergen, W.M. White, J.C. Varekamp, Sr–Nd–Pb isotope systematics of the Banda Arc, Indonesia: combined subduction and assimilation of continental material, *J. Geophys. Res.* 98 (1993) 22349–22366.
- [30] W. Todt, R.A. Cliff, A. Hanser, A.W. Hofmann, Evaluation of a ^{207}Pb – ^{205}Pb spike for high-precision lead isotope analysis, in: A. Basu, S.R. Hart (Eds.), *Earth Processes: Reading the Isotopic Code*. *Geophys. Monogr.*, 95 (1966) 429–437.
- [31] J. Hess, M.L. Bender, J.G. Schilling, Seawater $^{87}\text{Sr}/^{86}\text{Sr}$ evolution from Cretaceous to present, *Science* 231 (1986) 979–984.
- [32] D.A. Hodell, P.A. Mueller, J.R. Garrido, Variations in strontium isotopic compositions of seawater during the Neogene, *Geology* 19 (1991) 24–27.
- [33] R.B. Koepnick, W.H. Burke, R.E. Denison, E.A. Hetherington, H.F. Nelson, J.B. Otto, L.E. Waite, Construction of the seawater $^{87}\text{Sr}/^{86}\text{Sr}$ curve for the Cenozoic and Cretaceous: supporting data, *Chem. Geol.* 58 (1985) 55–81.
- [34] D.J. DePaolo, Detailed record of the Neogene Sr isotopic evolution of seawater from DSDP Site 590B, *Geology* 14 (1986) 103–106.
- [35] A.W. Mantyla, J.L. Reid, On the origins of deep and bottom waters of the Indian Ocean, *J. Geophys. Res.* 100 (1995) 2417–2439.
- [36] D.J. Piepgras, G.J. Wasserburg, Rare earth transport in the western North Atlantic inferred from isotopic observations, *Geochim. Cosmochim. Acta* 51 (1987) 1257–1271.
- [37] D.J. Piepgras, G.J. Wasserburg, E.G. Daseh, The isotopic composition of Nd in different ocean masses, *Earth Planet. Sci. Lett.* 45 (1979) 223–236.
- [38] D.J. Piepgras, S.B. Jacobsen, The isotopic composition of neodymium in the North Pacific, *Geochim. Cosmochim. Acta* 52 (1988) 1373–1381.
- [39] C. France-Lanord, L. Derry, A. Michard, Evolution of the Himalayas since Miocene time: isotopic and sedimentological evidence from the Bengal Fan, *Geol. Soc. London, Spec. Publ.* 74 (1991) 603–621.
- [40] C.J. Bertram, H. Elderfield, The geochemical balance of the rare-earth elements and neodymium isotopes in the oceans, *Geochim. Cosmochim. Acta* 57 (1993) 1957–1986.
- [41] L. Keigwin, Isotopic palaeoceanography of the Caribbean and East Pacific: role of Panama uplift in late Neogene time, *Science* 217 (1990) 203–234.
- [42] P.F. Barker, J. Burrell, The opening of the Drake Passage, *Mar. Geol.* 25 (1997) 15–34.
- [43] F. Woodruff, S.M. Savin, Miocene deep water oceanography, *Paleoceanography* 4 (1989) 87–140.